SEMARAK ILMU PUBLISHING

CFD Letters

Journal homepage:
https://semarakilmu.com.my/journals/index.php/CFD_Letters/index
ISSN: 2180-1363

Flow Behaviour and Wall Shear Stress Derivatives in Abdominal Aortic Aneurysm Models: A Detailed CFD Analysis into Asymmetry Effect

Djelloul Belkacemi[1,2], Mohammad Al-Rawi[3,*], Miloud Tahar Abbes[1], Boualem Laribi[4]

[1] Mechanics and Energetics Laboratory, Hassiba Ben Bouali University, Chlef, Algeria
[2] Unité de Développement des Equipements Solaires UDES, CDER, Bousmail, Tipaza, Algeria
[3] Center for Engineering and Industrial Design, Waikato Institute of Technology, Hamilton, New Zealand
[4] FIMA Laboratory, Djilali Bounaama University, Khemis Miliana, Ain Defla, Algeria

ARTICLE INFO

Article history:
Received 8 June 2022
Received in revised form 24 July 2022
Accepted 15 August 2022
Available online 30 September 2022

Keywords:
Hemodynamics; CFD; Abdominal Aortic Aneurysm; Geometry; Thrombus; Rupture.

ABSTRACT

Assessing the risk of rupture is extremely important to reduce the mortality of the abdominal aortic aneurysm (AAA). Current clinical guidelines suggest considering the maximum diameter as a criterion for planning and surgical intervention; however, this approach is too simplistic and overlooks other morphological parameters that are associated with the risk of rupture. The aim of this paper is to study the thrombogenicity and to predict the risk of AAA rupture by taking into consideration the geometrical asymmetry of the aneurysm, studying its effect on blood flow behaviour and vortical structure, spatiotemporal distribution of wall shear stresses (WSS), and their related parameters. To show the effect of asymmetry on blood flow dynamics and hemodynamic forces, five virtual models were constructed using five values of geometrical asymmetry ratio β ranging from β=0.2 (asymmetric model; AM) to β=1 (symmetric model; SM). Simulations were run for each geometry under transient physiological flow conditions using finite volume discretization. Resting flow rate was investigated in these models and our results demonstrate that the asymmetry of the aneurysm has a clear effect on the flow behaviour, and consequently on WSS distribution, oscillatory shear index (OSI) and time averaged wall shear stress (TAWSS). Furthermore, these preliminary findings suggest that thrombus formation and rupture risk are more probable in an asymmetric abdominal aortic aneurysm.

1. Introduction

Abdominal aortic aneurysm (AAA) is characterized by a deformation and a localized dilatation of the abdominal aorta (usually infrarenal) to at least one and a half times the diameter of the healthy aorta. AAA is one of the most common cardiovascular diseases, with a prevalence of 6-8 % for people over 65 years old, reaching up to 10% for 80 years old male subjects [1]. The average prevalence of AAA was 5.7% in the literature until February 2013 [2]. A complication of AAA is a sudden rupture, and this accounts for up to 4 to 5% of all sudden deaths according to Schermerhorn [3], and is ranked as the 14th most common cause of death in the world [4].

* *Corresponding author.*
E-mail address: mohammad.al-rawi@wintec.ac.nz (Al-Rawi Mohammad)

https://doi.org/10.37934/cfdl.14.9.6074

AAA is also characterized by a high mortality rate during and after surgery which prompted some authors to suggest that subgroups of patients might be excluded from surgery [5,6]. In the US, the incidences of AAAs reach up to 55,000/year and the incidence of AAA rupture is 10,000 [7]. Sakalihasan *et al.,* [8] reported that the number of deaths caused by ruptured aneurysms is about 8,000 and 15,000 patients in the UK and in the USA respectively.

Assessing the risk of rupture is extremely important in reducing AAA mortality. Currently, the most commonly used criterion to select eligible patients for surgery relies on the measurement of the AAA maximum diameter [9,10]. Surgery is recommended when the maximum diameter reaches 5.5 cm; however, many surgeons have observed that some AAAs became greater (11 or 12 cm) and remained unruptured, whilst others were smaller (<5.5cm) could break abruptly [11,12]. This evidence suggests there is a need to better stratify the risk for AAA rupture by determining additional criteria to help surgeons make clinical decisions regarding surgical intervention and management of patients with AAA.

Several researchers have studied the effect of aneurysm geometry and the mechanical behaviour of the wall on hemodynamic forces [13-15].The fact that AAA is often associated with deposition of blood clots and cell debris in the intraluminal thrombus (ILT), as well as the breakdown of connective tissue in the wall, which plays an important role in rupture and remodelling of the wall, makes the fluid dynamics in AAA, including the evolution of velocity and wall shear stress, a very promising index to improve prediction of AAA rupture.

Several numerical studies show that, compared to reconstructed geometries from medical imaging, virtual aneurysm models are more useful for parametrical studies [16,17]. The use of idealized geometry was adopted in many studies concerning AAA and other cardiovascular diseases [15-22]. The models do not preserve the physiologically correct geometry, but they still retain important physical processes that occur in an AAA [23].

Some numerical studies have been done on the hemodynamic characteristics of symmetric and asymmetric idealized models, and experimental modelling studies have been carried out by Salsac *et al.,* [17]. The study by Finol *et al.,* [25] was devoted to the understanding of the relation between the aneurysm asymmetry and the WSS distribution. In a study by Soudah *et al.,* [24], many geometric parameters including the asymmetry were tested.

In this work, the relationship between hemodynamic and WSS during the cardiac cycle for different symmetric and asymmetric geometries of aneurysm was studied. To the best of our knowledge, this is the first study to provide a detailed analysis in idealized symmetric and asymmetric aneurysms, including flow behaviour, WSS, vorticity, oscillatory shear index (OSI), and time averaged wall shear stress (TAWSS), which are very important factors for the understanding of thrombus formation and rupture risk evaluation.

2. Methodology

2.1 Geometries

The adopted geometries have a diameter of $\mathrm{d} = 2\,\mathrm{cm}$ in inlet and outlet, and a maximum diameter of $\mathrm{D} = \mathrm{DAAAmax} = 3\mathrm{d}$ in the median section of the AAA sac (see Figure 1). The asymmetry ratio β is:

$$\beta = \frac{r}{R} \tag{1}$$

where r is the radius measured at the medial section of an AAA sac from the longitudinal part toward the posterior part and R is the radius measured at the medial section of an AAA sac from the longitudinal part toward the anterior part. β=1 corresponds to a symmetric AAA.

The aneurysm lumen geometry is given by:

$$\varphi(z) = \begin{cases} d\left(\cos\left(\frac{\pi}{3d}(z-6d)+2\right)\right) & \begin{cases} 3d \le z < 9d \\ 0 \le z < 3d \; and \; 9d \le z < 12d \end{cases} \\ d \end{cases} \quad (2)$$

$$\delta(z) = \frac{3}{4}\left(\frac{1-\beta}{1+\beta}\right)(\varphi(z) - d) \quad (3)$$

Where $\varphi(z)$ define the diameter of the aneurysm sections along the aorta (axis z) and $\delta(z)$ define its deviation from the centre (Figure 1).

$\beta = \{0.2, 0.4, 0.6, 0.8, 1\}$ Has been considered, corresponding to five different geometries of AAA as proposed by Scotti *et al.,* [26].

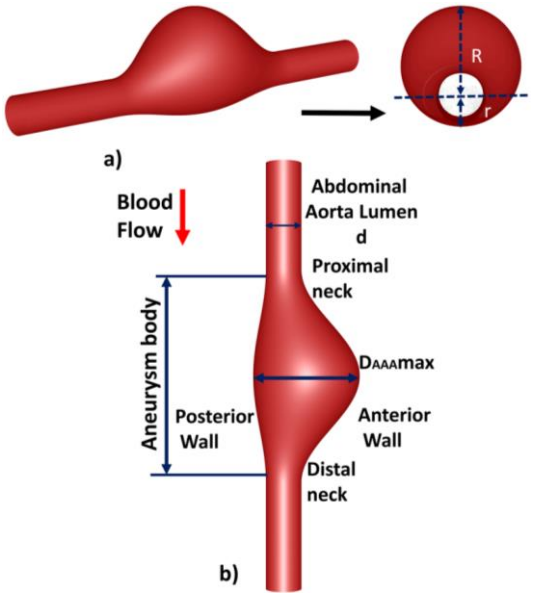

Fig. 1. Geometry of the AAA models (asymmetric model with asymmetry ratio β =0.4 is Model is illustrated) (a) Cross section (b) Vertical section

2.2 CFD Simulation

Mesh sensitivity studies were performed with the aim of defining the optimum computational domain for each AAA models. The software Gambit 2.4.6 (Ansys Inc.) was used for the mesh generation. For the symmetric model (SM), the mesh was changed from 886950 elements (1068637 nodes) to 1503607 elements (1777500 nodes), and from 888973 elements (1070657nodes) to 1475241 elements (1744138 nodes) for the AM. The resolution of the boundary layer, as shown in Figure 2(b), was adapted near the wall and the cell adjacent to the wall satisfied Eq. (4); this ensures accurate estimations of velocity gradients, and wall shear stresses near the wall. The optimum mesh size was determined once the peak wall shear stress does not increase by more than 2%. Based on this analysis, the final hexahedral meshes' grids were constructed (# β=0.2 (AM): 1,241,376 elements; # β=0.4: 1,204,320; # β=0.6: 1,176,528; # β=0.8: 1,162,632; # β=1 (SM): 1,148,736).

$$y_p\sqrt{\frac{v_\infty}{\upsilon\, x}} \leq 1 \tag{4}$$

where y_p is the distance between the wall and centre of the adjacent mesh cell, v_∞ is the free-stream velocity, υ is the kinematic viscosity of the fluid and x is the distance along the wall from the starting point of the boundary layer.

The workstation used to perform the simulations in this work is with two Xeon E5-2660 processors and 16 GB of RAM. The run time was 69 hours and 33 minutes for each cardiac cycle in the case of the SM, and approximately 81 hours and 9 minutes for the AM. Five cardiac cycles were simulated to minimize the influence of initial conditions, and the last cycle was considered in our results.

A no-slip boundary condition was imposed at the wall supposing that it is rigid. In fact, the wall of the AAAs become stiffer following the loss of elastin and their compliance is nearly negligible compared to a healthy aorta [27,28]. This hypothesis was adopted in many studies concerning aorta and AAA [20,21,29-34].

At the geometry inlet, a pulsatile velocity is applied (Figure 2(a)) which is justified by the fact that this condition is applied to the unexpanded section of the anterior portion of the abdominal aorta and a free pressure boundary condition was imposed at the geometry outlet. These hemodynamic conditions were referred to in previous studies [25,35]. The temporal variations of these physiological velocity inlet condition were reproduced by Fourier series of order 16th for velocity and implemented through a User_Defined_Function (UDF) script.

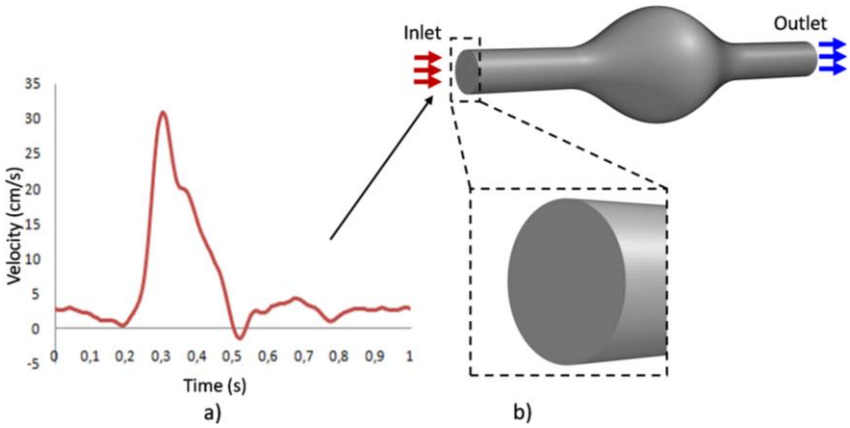

Fig. 2. Boundary conditions (a) Velocity waveform and (b) Boundary layer mesh (SM β =1 is illustrated)

In order to avoid numerical instabilities, the inlet and outlet boundaries were extended by three times the diameter of the healthy part of the aorta (Figure 1). The natural frequency of the pulsatile flow is set to $\omega = 2\pi\ \mathrm{rad/s}$, with a period $T = 1\mathrm{s}$.

2.3 Governing Equations

Even if blood is a suspension of cells in plasma, in large-sized vessels, the non-Newtonian behaviour of blood is limited, and it begins to play a role in vessels smaller than 1 mm in diameter [35-37]. Pedley and Fung [38] shows that in vessels greater than approximately 0.5 mm in diameter it is reasonable to model blood as a Newtonian fluid.

This assumption was adopted in most of the previous works, where blood is considered as an incompressible and Newtonian fluid, with a homogeneous dynamic viscosity of 0.0035 $Pa.s$, and density of 1,050 kg/m^3 [30,39]. The flow in the abdominal aorta is hence described by the incompressible Navier-Stokes equations:

$$\rho \frac{\mathrm{dv}}{\mathrm{dt}} = -\nabla \mathrm{p} + \mu\, \Delta \mathrm{v} \tag{5}$$

$$\nabla . \mathrm{v} = 0 \tag{6}$$

Where ρ is the density of the blood, p is the pressure of the blood and μ is dynamic viscosity of the blood.

In this study the Finite Volume Method (FVM) was adopted to solve the governing equations and to predict the time-dependent flow through three-dimensional abdominal aortic aneurysm geometry by using Fluent (Ansys, Inc.) with the implicit solver. A second-order upwind scheme was used for spatial discretization and the PISO (implicit operator splitting pressure) algorithm for pressure-velocity coupling. The time-step size was taken equal to 10^{-3}s, which is equivalent to 1000 time-steps for each cardiac cycle using the iterative time advancement scheme. The convergence criteria for the continuity and the velocity are in the order of 10^{-6} and 10^{-5}, respectively.

2.4 Wall Parameters' Analysis

Many hemodynamic wall parameters including WSS and OSI, and TAWSS were documented [40]. An in-house MATLAB code (The Mathworks Inc.) was used for the post-processing and the calculation of those parameters [41].

In detail, WSS is defined as:

$$\mathrm{wss} = \mu \left(\frac{\partial \mathrm{v}}{\partial \mathrm{y}}\right)_{\mathrm{y}=0} \tag{7}$$

where y Is the distance to the wall.

OSI represents the temporal variation in WSS direction which has been shown to affect the endothelial cells' behaviour and vessel wall thickness. It is defined as:

$$\mathrm{OSI} = \frac{1}{2}\left(1 - \frac{\left|\int_0^{\mathrm{T}} \mathrm{wss}\ \mathrm{dt}\right|}{\int_0^{\mathrm{T}} |\mathrm{wss}|\ \mathrm{dt}}\right) \tag{8}$$

where $\left|\int_0^{\mathrm{T}} \mathrm{wss}\ \mathrm{dt}\right|$ is the magnitude of time-Averaged WSS (TAWSS) vector. TAWSS is defined as:

$$\mathrm{TAWSS} = \int_0^{\mathrm{T}} |\mathrm{wss}|\ \mathrm{dt} \tag{9}$$

2.5 CFD Validation

To validate our numerical model, we performed a comparison of the axial velocity profile at the centre of the aneurysm with the experimental and numerical data of Budwig *et al.,* [42] for steady flow through the axisymmetric AAA model (as shown in Figure 3(b) and Figure 3(c)). The simulations are carried out at Re = 400, aneurysm-to-artery diameter ratio D/d=2.1, and an aspect ratio of the

aneurysm L/d=4 (L is the length of the aneurysm). The results generated in the present numerical simulation show good agreement with the experimental and numerical results [42]. The flow feature characterized by the formation recirculating vortex was in agreement with in vitro studies (as shown in Figure 3(b)) [42]. The shape of the aneurysm was not detailed in a study by Budwig *et al.,* [42]. The slight difference in our velocity profile (in which the dome of the profile is slightly larger) compared could be due to the possible difference in the shape of our aneurysm, experimental and numerical results [42].

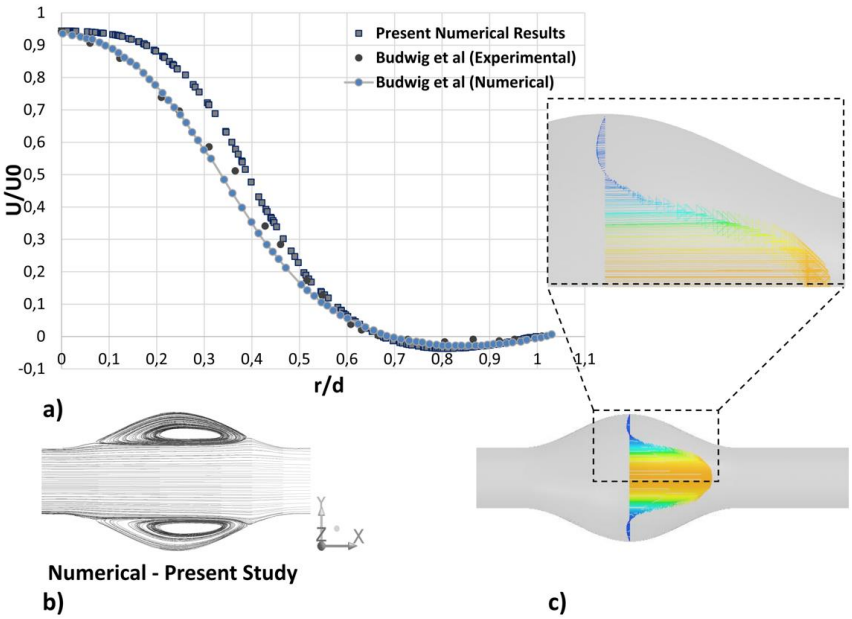

Fig. 3. Model with Re=500, R⁄r0 = 2.1 and L⁄r0 = 8. (a) Comparison of steady profile across the centre of the AAA with experimental and numerical results, (b) Streamlines using present numerical model and (c) Profile across the centre of the AAA

3. Results

3.1 Flow Behaviour in an AAA

Figure 4(a) shows the general features characteristics of the flow with reference to the symmetric aneurysm (β= 1). At the inlet of the aneurysm (distal neck), a jet is formed and enters into the aneurysmal sac; this result is in perfect agreement with the experimental results of Deplano *et al.,* [43]. The velocity gradient between the jet flow and the surrounding parts produces shear layers, generating vortices detected in the horizontal and vertical vorticity contours and in velocity vectors (see Figure 4 and Figure 5).

The general characteristics of the flow in our results, the vortex formation, the impingement of the jet and regions of high and low WSS, are in good agreement with those in prior experimental studies [23,43].

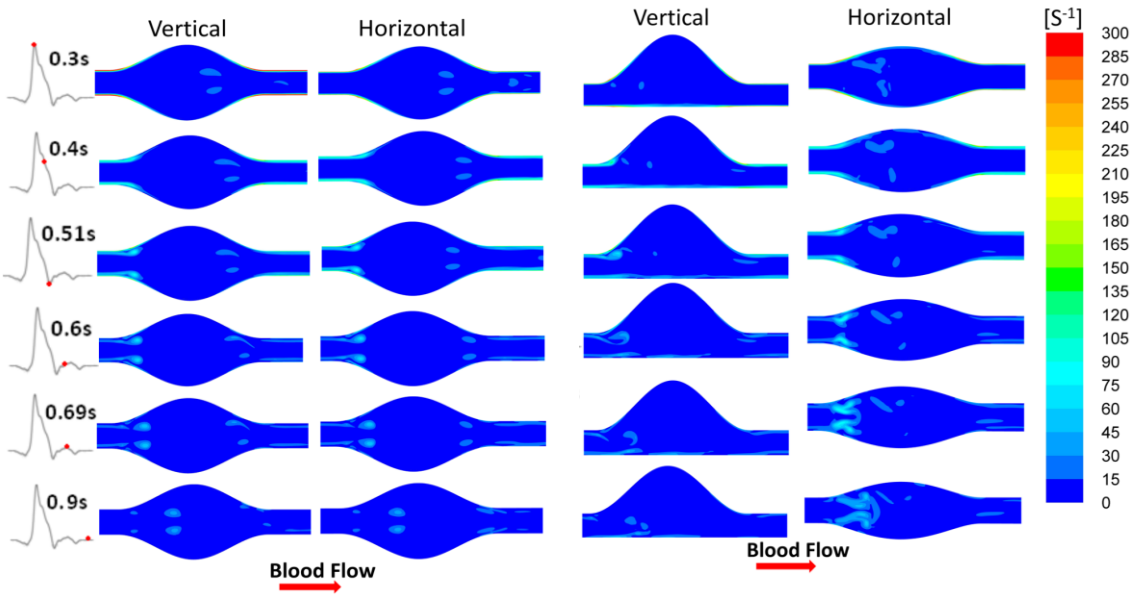

Fig. 4. Vorticity temporal evolution [s-1] for (a) Symmetric Model (SM) and (b) Asymmetric Model (AM), in vertical and horizontal planes respectively

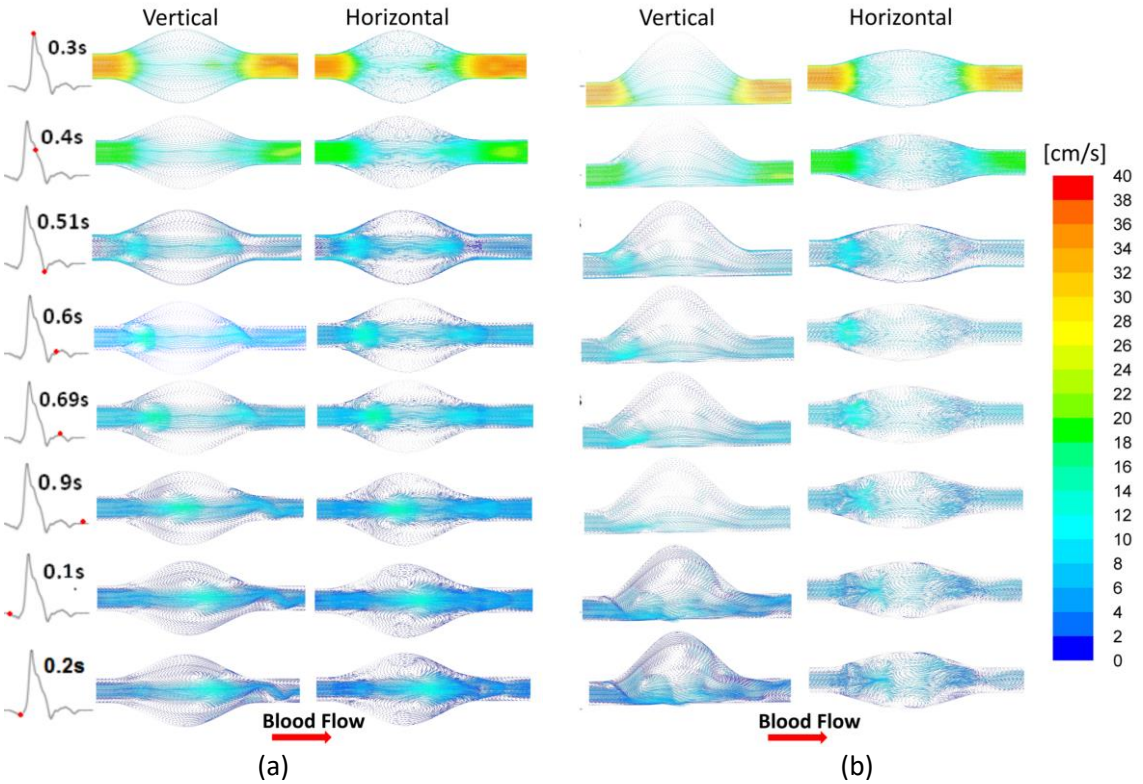

Fig. 5. Velocity vectors temporal evolution [cm/s] for (a) Symmetric Model (SM) and (b) Asymmetric Model (AM), in vertical and horizontal planes respectively

3.2 Flow Dynamics and Vortical Structure Discussion

The effect of the asymmetry on the flow patterns and vortical structures is shown in Figure 6 where the time evolution of 3D vortical structures by the isosurfaces of $\lambda 2$-Criterion Jeong and Hussain [44] is reported.

According to the results presented in the previous section, the aneurysm asymmetry is directly proportional to the earlier separation of the flow, and the vortex occurring in asymmetric aneurysms persist for a longer period compared to those occurring in symmetric aneurysms; in particular, these vortices persist throughout the cardiac cycle for the completely AM. This persistence is due to the separation of the fluid caused by the abrupt change of the section creating areas with large velocity gradients, the velocity gradient produces a stronger vortex. For the AM, the vortices which are produced during the deceleration phase are still present at the diastolic peak and roll-up from the proximal neck (enlargement) impinging on the distal neck (narrowing) (see Figure 6).

In the SM, the vortex ring (VR) starts from the proximal neck during the acceleration phase and is transported along the bulb of the aneurysm to the distal neck. The shape of the VR is conserved and does not change until the end of the cycle. A different behaviour is observed in the Figure 5(b), which represents the temporal evolution of the vortex structure in the case of an AM. In the asymmetric aneurysm, the vortex core spreads across the bulb and impacts the distal/anterior wall forming fluctuation zones.

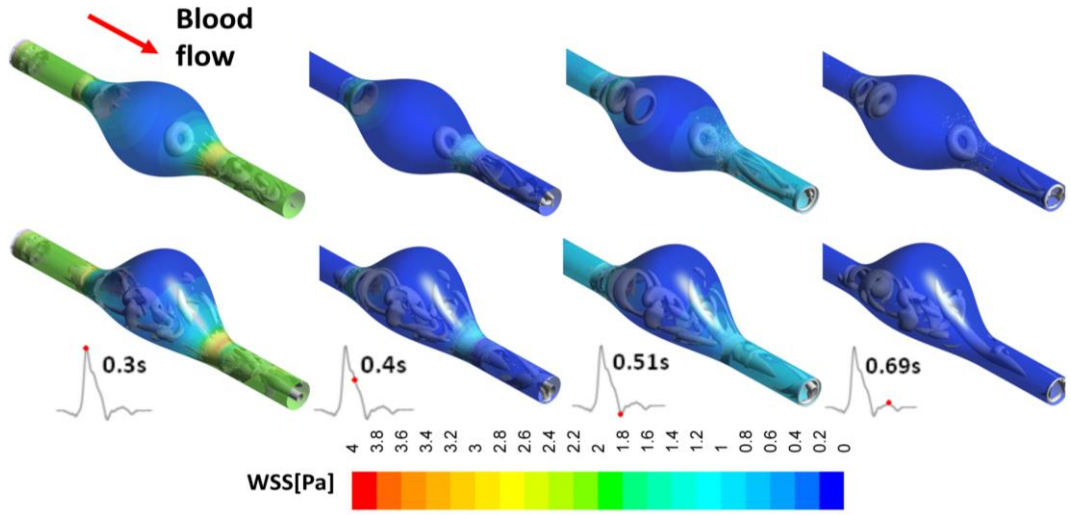

Fig. 6. Temporal iso-surfaces of $\lambda 2$-Criterion with threshold value of -10 [s^{-2}] with wall coloured by WSS [Pa] at t=0.3, 0.4, 0.51 and 0.69 respectively from left to right. [SM: upper line and AM: Lower line]

As shown in Figure 7, in the case of AM with symmetry factor equal to 0.6, the VR starts to form at t=0.3s (systolic peak) in the proximal neck, and its shape becomes complete at t=0.45s. Considering this time frame as the starting instant of the VR, Figure 7 demonstrates its persistence until the same time frame of the next cardiac cycle; however, its shape is lost at t=0.3s and the ring opens close to the posterior wall. This evidence confirms that the shape and the persistence of the VR are in an inverse relationship with the asymmetry of the aneurysm.

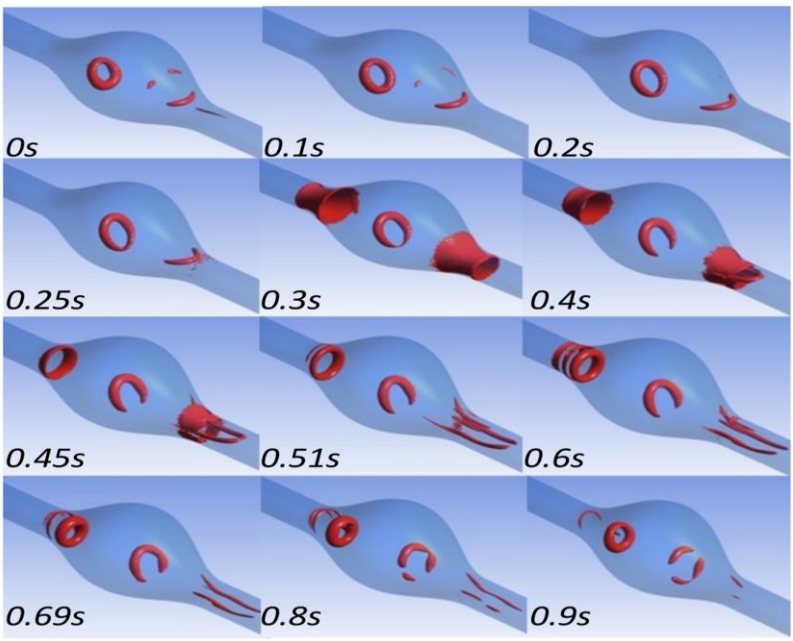

Fig. 7. Temporal iso-surfaces of swirling strength using a threshold value of 10 [s^{-1}] for the model β = 0.6

3.3 Wall Shear Stress Analysis

In addition to the endothelial layers' thrombogenic function, they are also the mechano-detecting elements which detect the local blood flow conditions and induce autocrine stimulation. In vivo and in vitro studies demonstrate the destructive effect of low and oscillatory WSS on the endothelial function and their effect on intimal thickening [37,45]. Under physiologic shear stress, the endothelial cells are aligned to the flow direction, which differs from the low shear stress case [37,46]. Regions of low WSS are also associated with rupture and expansion sites of the AAAs [47,48]. The high level of WSS leads to athero-protective endothelial phenotype and decreases the expression of the vasoconstrictor [37].

Figure 8 and Figure 9 show the contours of WSS in the SM and AM across three instances of the cardiac cycle. By analysing these figures, it can be observed that during systolic acceleration, WSSs are greater in the healthy part of the aorta (the unexpanded part) than in the wall of the aneurysm sac, which remains in this condition until it reaches WSS-max at the systolic peak t=0.3s; this observation is valid both for symmetric and asymmetric aneurysm models. The distal and proximal necks are subjected to very high WSS, in contrast to the sac of the aneurysm where low WSS occur. During the deceleration phase, the WSS-max values are still in the two necks, and this configuration persists for the remaining period of the cardiac cycle (see Figure 8(a) and Figure 8(b) at t=0.69s).

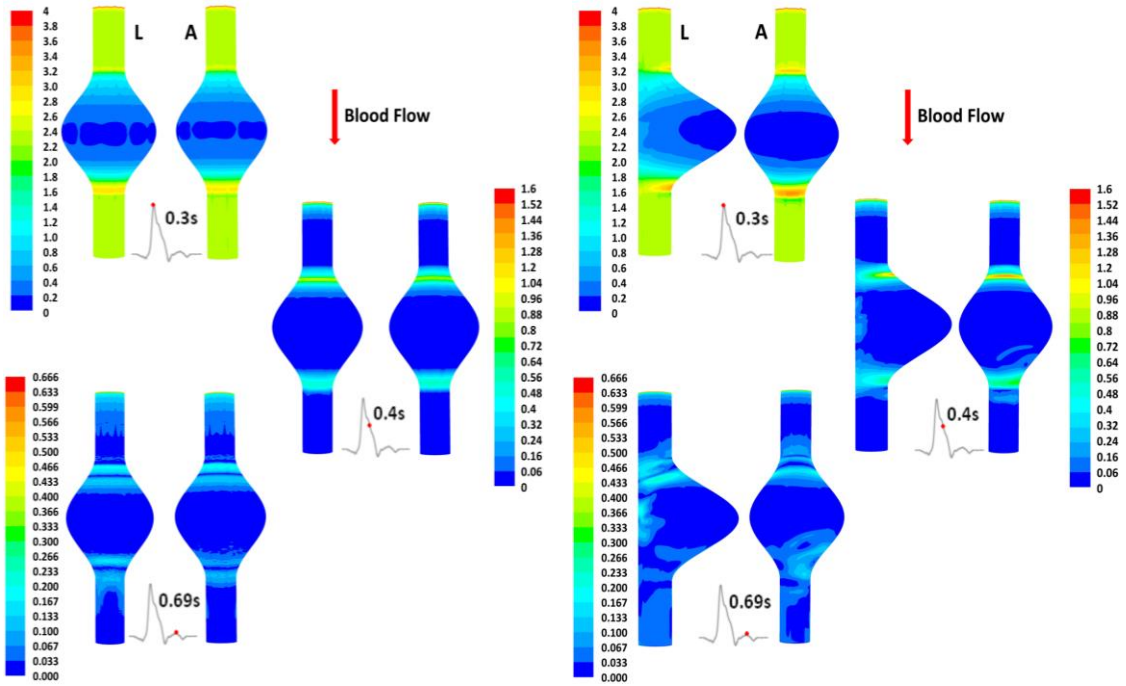

(a) (b)

Fig. 8. WSS contours [Pa] in vertical and horizontal plane respectively in (a) SM and (b) AM: at t=0.3s systolic peak, at t=0.4s and at diastolic peak t=0.69s

Figure 9(a) to Figure 9(f) show the time evolution of WSS in the five aneurysm models. By analysing this figure, it can be observed that the WSS curvature in the proximal neck is almost the same in the anterior wall represented by P1 (Figure 9(a)), and in the posterior wall, represented by P1' (Figure 9(b)). In the aneurysm sac, the anterior wall (Figure 9(c)) is subjected to WSSs that are lower than those experienced by the posterior wall (Figure 9(d)); also, in this case, the WSS-max becomes lower on the anterior wall when the level of asymmetry increases. By contrast, in the distal neck, the WSSs are highest in the anterior wall (Figure 9(e)) than in the posterior one (Figure 9(f)).

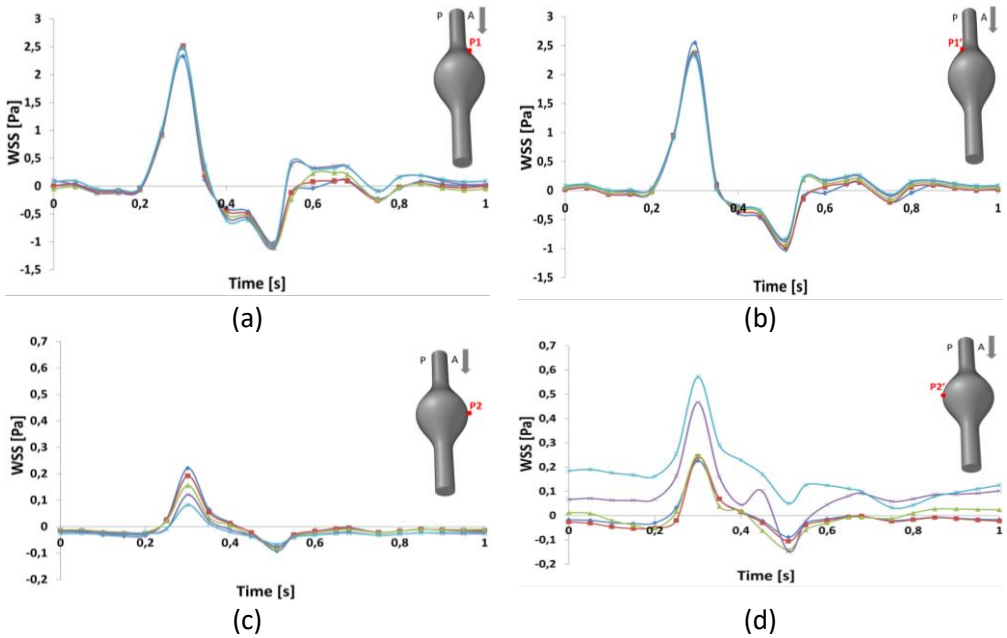

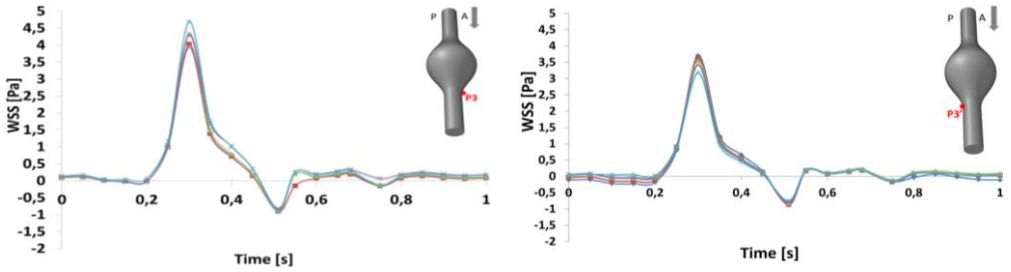

(e) (f)

Fig. 9. WSS temporal evolution [Pa] in the models (β=1 β=0.8 β=0.6 β=0.4 β=0.2.), (a) in proximal neck / anterior wall (P1), (b) in proximal neck / posterior wall (P1'), (c) In sac / anterior wall point (P2), (d) in sac / posterior wall (P2'), (e) In distal neck / anterior wall (P3), (f) in distal neck / posterior wall (P3')

3.4 Analysis of TAWSS and OSI

Figure 10 and Figure 11 respectively show the InvTAWSS and OSI for the SM and the AM (InvTAWSS the inverse of the TAWSS is displayed for visualization purpose to better detect regions of low TAWSS). The posterior, anterior, left and right views are shown.

The OSI contours (see Figure 11) in the AAA models predict similar behaviour featured by high values in the aneurysm sac. High OSI values are encountered at the wall part near to the recirculation zones. Although these values reach the maximum (OSI≈0.5) in some regions the case of AM in the anterior part of the wall, this region is subjected to the vortices which were seen earlier in section 3.2. An OSI close to 0.5 indicates a region with completely oscillating WSS. In the SM the entire sac is subjected to oscillating WSS (High OSI values), this could be related to the vortex ring detected in this model. The TAWSS in this model is higher than the AM (InvTAWSS reaches highest values in the asymmetric model AM compared to the symmetric model SM as shown in Figure 10).

Regions where large OSI and small TAWSS (High InvTAWSS) are concomitant, indicate an elevated thrombogenic susceptibility. Da Silva *et al.,* [49] report that ruptures occurred in the region of intraluminal thrombus (ILT) in 80% of AAA.

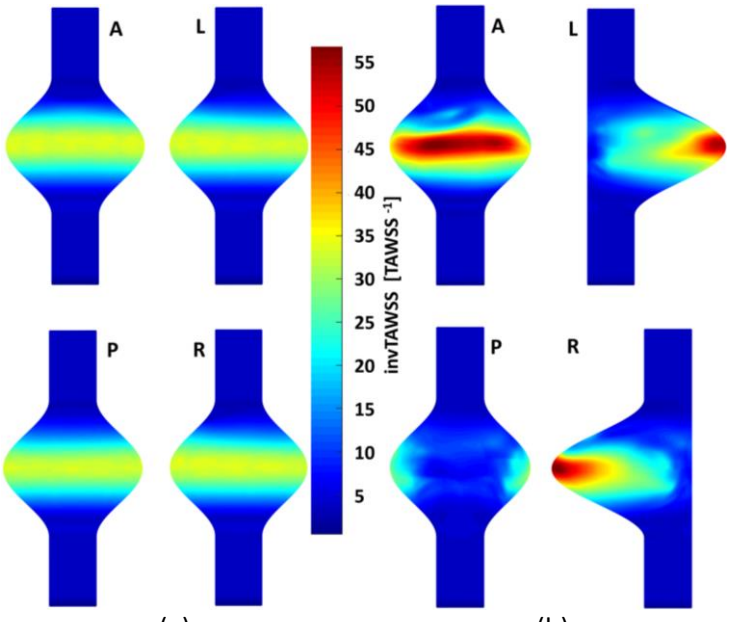

(a) (b)

Fig. 10. InvTAWSS contours [Pa-1] in SM (left column) AM (left column) [(Views :P: posterior, A: anterior, L: left, R: right)]

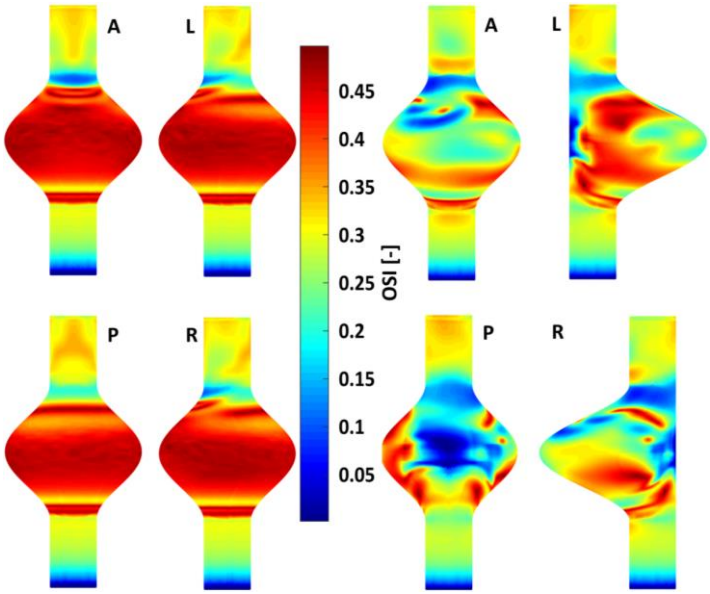

Fig. 11. OSI contours [-] in SM (left column) AM (left column) [(Views :P: posterior, A: anterior, L: left, R: right)]

The notion of minimum values of the WSS has significant effect on the rupture of abdominal aortic aneurysm Boyd *et al.,* [47]. The low values of WSSs are observed in the aneurysm sac where recirculation zones have appeared. The asymmetry of the aneurysm has a clear effect on the flow behaviour, the recirculation zones formation and consequently on WSS and its derivatives distribution recent studies. Previous studies were devoted to the understanding of the relationship between vortical structure and ILT accumulation and WSS derivatives showing the importance of CFD as possible tool to help clinicians [50].

4. Conclusions

In this study, a detailed parametric analysis of flow dynamics using five virtual AAA models was performed numerically; the spatial distribution and the temporal evolution of wall shear stresses were also studied. In addition, hemodynamic parameters such as OSI and TAWSS were analysed to define the effect of AAA asymmetry on a possible risk of rupture and on the promotion of thrombus formation.

The general characteristics of flow in AAA can be summarized by the formation of a jet that enters the aneurysm, which velocity gradient with respect to the surrounding stationary flow area generates shear layers that evolve creating vortices. Importantly, the development of these vortices is highly influenced by the symmetry of the aneurysm: in the case of an asymmetrical aneurysm, the vortex persists longer than in a symmetrical one. These changes, compared to the flow characteristics in a healthy artery, result in significant changes in the spatial and temporal distribution of wall shear stresses that act on the endothelial cells.

The presented results show that the aneurysm is also subjected to low and oscillating wall shear stresses, with an OSI close to 0.5 in the case of an SM in the entire aneurysm sac. Such conditions favour intraluminal thrombus (ILT) formation and endothelial dysfunction. The results of this detailed CFD study confirm that the asymmetry of the abdominal aortic aneurysm potentially increases its likelihood of rupture and the ILT formation. Although the studied symmetric and asymmetric AAA models have an equal maximum diameter, the asymmetry of AAA has a clear impact on the flow

behaviour and WSS derivatives values which could favour their susceptibility to rupture and the formation of ILT.

Despite the limitations of our study, our results provide an interesting data for the understanding of the hemodynamic properties in AAAs, and how CFD study could be useful for clinicians in the prediction of the likelihood of AAA rupture. This study needs to be enlarged to a cohort of patients with ruptured and unruptured AAAs in order to validate its impact on the improvement of risk stratifications due to flow-derived biomechanical bio-markers.

Acknowledgement
The authors would like to thank the DGRSDT Algiers (Direction Générale de la Recherche Scientifique et du Développement Technologique, Algiers) for its contribution to this article.

References

[1] Cosford, Paul A., Gillian C. Leng, and Justyn Thomas. "Screening for abdominal aortic aneurysm." *Cochrane Database of Systematic Reviews* 2 (2007). https://doi.org/10.1002/14651858.CD002945.pub2

[2] Stather, P. W., D. A. Sidloff, I. A. Rhema, E. Choke, M. J. Bown, and R. D. Sayers. "A review of current reporting of abdominal aortic aneurysm mortality and prevalence in the literature." *European Journal of Vascular and Endovascular Surgery* 47, no. 3 (2014): 240-242. https://doi.org/10.1016/j.ejvs.2013.11.007

[3] Schermerhorn, Marc. "A 66-year-old man with an abdominal aortic aneurysm: review of screening and treatment." *JAMA* 302, no. 18 (2009): 2015-2022. https://doi.org/10.1001/jama.2009.1502

[4] Bouferrouk, A., S. Boutamine, and A. Mekarnia. "Dépistage opportuniste de l'anévrisme de l'aorte abdominale lors d'une écho-cardiographie transthoracique chez des patients sélectionnés: expérience d'un centre algérien." *Journal des Maladies Vasculaires* 40, no. 5 (2015): 312. https://doi.org/10.1016/j.jmv.2015.07.101

[5] Hallin, A., David Bergqvist, and Lars Holmberg. "Literature review of surgical management of abdominal aortic aneurysm." *European Journal of Vascular and Endovascular Surgery* 22, no. 3 (2001): 197-204. https://doi.org/10.1053/ejvs.2001.1422

[6] Scheer, Margot LJ, Robert A. Pol, Jan Willem Haveman, Ignace FJ Tielliu, Eric LG Verhoeven, Jan JAM Van Den Dungen, Maarten W. Nijsten, and Clark J. Zeebregts. "Effectiveness of treatment for octogenarians with acute abdominal aortic aneurysm." *Journal of Vascular Surgery* 53, no. 4 (2011): 918-925. https://doi.org/10.1016/j.jvs.2010.10.072

[7] McPhee, James T., Joshua S. Hill, and Mohammad H. Eslami. "The impact of gender on presentation, therapy, and mortality of abdominal aortic aneurysm in the United States, 2001-2004." *Journal of Vascular Surgery* 45, no. 5 (2007): 891-899. https://doi.org/10.1016/j.jvs.2007.01.043

[8] Sakalihasan, Natzi, Raymond Limet, and Olivier Damien Defawe. "Abdominal aortic aneurysm." *The Lancet* 365, no. 9470 (2005): 1577-1589. https://doi.org/10.1016/S0140-6736(05)66459-8

[9] Doyle, Barry J., Anthony Callanan, Paul E. Burke, Pierce A. Grace, Michael T. Walsh, David A. Vorp, and Timothy M. McGloughlin. "Vessel asymmetry as an additional diagnostic tool in the assessment of abdominal aortic aneurysms." *Journal of Vascular Surgery* 49, no. 2 (2009): 443-454. https://doi.org/10.1016/j.jvs.2008.08.064

[10] Vorp, David A. "Biomechanics of abdominal aortic aneurysm." *Journal of Biomechanics* 40, no. 9 (2007): 1887-1902. https://doi.org/10.1016/j.jbiomech.2006.09.003

[11] Chaikof, Elliot L., David C. Brewster, Ronald L. Dalman, Michel S. Makaroun, Karl A. Illig, Gregorio A. Sicard, Carlos H. Timaran, Gilbert R. Upchurch, and Frank J. Veith. "The care of patients with an abdominal aortic aneurysm: the Society for Vascular Surgery practice guidelines." *Journal of Vascular Surgery* 50, no. 4 (2009): S2-S49. https://doi.org/10.1016/j.jvs.2009.07.002

[12] Hong, Lim Sheh, Mohd Azrul Hisham Mohd Adib, Mohd Shafie Abdullah, Nur Hartini Mohd Taib, Radhiana Hassan, and Azian Abd Aziz. "Study of extracted geometry effect on patient-specific cerebral aneurysm model with different threshold coefficient (Cthres)." *CFD Letters* 12, no. 10 (2020): 1-14. https://doi.org/10.37934/cfdl.12.10.114

[13] Vande Geest, Jonathan P., David E. Schmidt, Michael S. Sacks, and David A. Vorp. "The effects of anisotropy on the stress analyses of patient-specific abdominal aortic aneurysms." *Annals of Biomedical Engineering* 36, no. 6 (2008): 921-932. https://doi.org/10.1007/s10439-008-9490-3

[14] Raut, Samarth S., Santanu Chandra, Judy Shum, and Ender A. Finol. "The role of geometric and biomechanical factors in abdominal aortic aneurysm rupture risk assessment." *Annals of Biomedical Engineering* 41, no. 7 (2013): 1459-1477. https://doi.org/10.1007/s10439-013-0786-6

[15] Drewe, Corey J., Louis P. Parker, Lachlan J. Kelsey, Paul E. Norman, Janet T. Powell, and Barry J. Doyle. "Haemodynamics and stresses in abdominal aortic aneurysms: A fluid-structure interaction study into the effect of proximal neck and iliac bifurcation angle." *Journal of Biomechanics* 60 (2017): 150-156. https://doi.org/10.1016/j.jbiomech.2017.06.029

[16] Peattie, Robert A., Tiffany J. Riehle, and Edward I. Bluth. "Pulsatile flow in fusiform models of abdominal aortic aneurysms: flow fields, velocity patterns and flow-induced wall stresses." *Journal of Biomechanical Engineering* 126, no. 4 (2004): 438-446. https://doi.org/10.1115/1.1784478

[17] Salsac, Anne-Virginie, Steven R. Sparks, and Juan C. Lasheras. "Hemodynamic changes occurring during the progressive enlargement of abdominal aortic aneurysms." *Annals of Vascular Surgery* 18, no. 1 (2004): 14-21. https://doi.org/10.1007/s10016-003-0101-3

[18] Deplano, Valérie, Clark Meyer, Carine Guivier-Curien, and Eric Bertrand. "New insights into the understanding of flow dynamics in an in vitro model for abdominal aortic aneurysms." *Medical Engineering & Physics* 35, no. 6 (2013): 800-809. https://doi.org/10.1016/j.medengphy.2012.08.010

[19] Algabri, Yousif A., Surapong Chatpun, and Ishkrizat Taib. "An investigation of pulsatile blood flow in an angulated neck of abdominal aortic aneurysm using computational fluid dynamics." *Journal of Advanced Research in Fluid Mechanics and Thermal Sciences* 57, no. 2 (2019): 265-274.

[20] Jafarzadeh, Sina, Arsalan Nasiri Sadr, Ehsan Kaffash, Sahar Goudarzi, Ehsan Golab, and Arash Karimipour. "The effect of hematocrit and nanoparticles diameter on hemodynamic parameters and drug delivery in abdominal aortic aneurysm with consideration of blood pulsatile flow." *Computer Methods and Programs in Biomedicine* 195 (2020): 105545. https://doi.org/10.1016/j.cmpb.2020.105545

[21] Hegde, Pranav, Gowrava Shenoy B., A. B. V. Barboza, S. M. Abdul Khader, Raghuvir Pai, Masaaki Tamagawa, Ravindra Prabhu, and D. Srikanth Rao. "Numerical Analysis on A Non-Critical Stenosis in Renal Artery." *Journal of Advanced Research in Fluid Mechanics and Thermal Sciences* 88, no. 3 (2021): 31-48. https://doi.org/10.37934/arfmts.88.3.3148

[22] Wen, Jun, Ding Yuan, Qingyuan Wang, Yao Hu, Jichun Zhao, Tinghui Zheng, and Yubo Fan. "A computational simulation of the effect of hybrid treatment for thoracoabdominal aortic aneurysm on the hemodynamics of abdominal aorta." *Scientific Reports* 6, no. 1 (2016): 1-9. https://doi.org/10.1038/srep23801

[23] Salsac, A-V., S. R. Sparks, J-M. Chomaz, and J. C. Lasheras. "Evolution of the wall shear stresses during the progressive enlargement of symmetric abdominal aortic aneurysms." *Journal of Fluid Mechanics* 560 (2006): 19-51. https://doi.org/10.1017/S002211200600036X

[24] Soudah, E., G. Vilalta, M. Bordone, F. Nieto, J. A. Vilalta, and C. Vaquero. "Estudio paramétrico de tensiones hemodinámicas en modelos de aneurismas de aorta abdominal." *Revista Internacional de Métodos Numéricos para Cálculo y Diseño en Ingeniería* 31, no. 2 (2015): 106-112. https://doi.org/10.1016/j.rimni.2014.02.003

[25] Finol, E. A., K. Keyhani, and C. H. Amon. "The effect of asymmetry in abdominal aortic aneurysms under physiologically realistic pulsatile flow conditions." *Journal of Biomechanical Engineering* 125, no. 2 (2003): 207-217. https://doi.org/10.1115/1.1543991

[26] Scotti, Christine M., Alexander D. Shkolnik, Satish C. Muluk, and Ender A. Finol. "Fluid-structure interaction in abdominal aortic aneurysms: effects of asymmetry and wall thickness." *Biomedical Engineering Online* 4, no. 1 (2005): 1-22. https://doi.org/10.1186/1475-925X-4-64

[27] Di Achille, P., G. Tellides, C. A. Figueroa, and J. D. Humphrey. "A haemodynamic predictor of intraluminal thrombus formation in abdominal aortic aneurysms." *Proceedings of the Royal Society A: Mathematical, Physical and Engineering Sciences* 470, no. 2172 (2014): 20140163. https://doi.org/10.1098/rspa.2014.0163

[28] Seman, Che Mohammad Hafizal Muzammil Che, Nur Ayuni Marzuki, Nofrizalidris Darlis, Noraini Marsi, Zuliazura Mohd Salleh, Izuan Amin Ishak, Ishkrizat Taib, and Safra Liyana Sukiman. "Comparison of Hemodynamic Performances Between Commercial Available Stents Design on Stenosed Femoropopliteal Artery." *CFD Letters* 12, no. 7 (2020): 17-25. https://doi.org/10.37934/cfdl.12.7.1725

[29] Zambrano, Byron A., Hamidreza Gharahi, ChaeYoung Lim, Farhad A. Jaberi, Jongeun Choi, Whal Lee, and Seungik Baek. "Association of intraluminal thrombus, hemodynamic forces, and abdominal aortic aneurysm expansion using longitudinal CT images." *Annals of Biomedical Engineering* 44, no. 5 (2016): 1502-1514. https://doi.org/10.1007/s10439-015-1461-x

[30] Piatti, F., D. Belkacemi, A. Caimi, F. Sturla, A. Greiser, F. Pluchinotta, and A. Redaelli. "On the potential of 4D Flow in guiding CFD analyses: a case study of aortic coartaction." In *Proceedings VII Meeting Italian Chapter of the European Society of Biomechanics (ESB-ITA 2017)*, pp. 28-29. 2017.

[31] Stefanov, Florian, Sherif Sultan, Liam Morris, Ala Elhelali, Edel P. Kavanagh, Violet Lundon, Mohamed Sultan, and Niamh Hynes. "Computational fluid analysis of symptomatic chronic type B aortic dissections managed with the Streamliner Multilayer Flow Modulator." *Journal of Vascular Surgery* 65, no. 4 (2017): 951-963. https://doi.org/10.1016/j.jvs.2016.07.135

[32] Khader, Shah Mohammed Abdul, Adi Azriff, Raghuvir Pai, Mohammed Zubair, Kamarul Arifin Ahmad, Zanuldin Ahmad, and Koteshwara Prakashini. "Haemodynamics study in subject-specific abdominal aorta with renal bifurcation using CFD-a case study." *Journal of Advanced Research in Fluid Mechanics and Thermal Sciences* 50, no. 2 (2018): 118-121.
[33] Zakaria, Mohamad Shukri, Farzad Ismail, Masaaki Tamagawa, Ahmad Fazli Abdul Azi, Surjatin Wiriadidjaya, Adi Azrif Basri, and Kamarul Arifin Ahmad. "Computational fluid dynamics study of blood flow in aorta using OpenFOAM." *Journal of Advanced Research in Fluid Mechanics and Thermal Sciences* 43, no. 1 (2018): 81-89.
[34] Mills, C. J., I. T. Gabe, J. H. Gault, D. T. Mason, J. Ross Jr, E. Braunwald, and J. P. Shillingford. "Pressure-flow relationships and vascular impedance in man." *Cardiovascular Research* 4, no. 4 (1970): 405-417. https://doi.org/10.1093/cvr/4.4.405
[35] Abbas, M. Ali, Y. Q. Bai, M. M. Rashidi, and M. M. Bhatti. "Application of drug delivery in magnetohydrodynamics peristaltic blood flow of nanofluid in a non-uniform channel." *Journal of Mechanics in Medicine and Biology* 16, no. 04 (2016): 1650052. https://doi.org/10.1142/S0219519416500524
[36] Al-Azawy, Mohammed Ghalib, Saleem Khalefa Kadhim, and Azzam Sabah Hameed. "Newtonian and non-newtonian blood rheology inside a model of stenosis." *CFD Letters* 12, no. 11 (2020): 27-36. https://doi.org/10.37934/cfdl.12.11.2736
[37] Westerhof, Nicolaas, Nikos Stergiopulos, Mark I. M. Noble, and Berend E. Westerhof. *Snapshots of hemodynamics: an aid for clinical research and graduate education*. New York: Springer, 2019. https://doi.org/10.1007/978-3-319-91932-4
[38] Pedley, Timothy J., and Y. C. Fung. "The fluid mechanics of large blood vessels." *Journal of Biomechanical Engineering* 102, no. 4 (1980): 345. https://doi.org/10.1115/1.3138235
[39] Ramakrishnan, K., and K. Shailendhra. "Hydromagnetic blood flow through a uniform channel with permeable walls covered by porous media of finite thickness." *Journal of Applied Fluid Mechanics* 6, no. 1 (2013): 39-47. https://doi.org/10.36884/jafm.6.01.19479
[40] He, Xiaoyi, and David N. Ku. "Pulsatile flow in the human left coronary artery bifurcation: average conditions." *Journal of Biomechanical Engineering* 118, no. 1 (1996): 74-82. https://doi.org/10.1115/1.2795948
[41] Himburg, Heather A., Deborah M. Grzybowski, Andrew L. Hazel, Jeffrey A. LaMack, Xue-Mei Li, and Morton H. Friedman. "Spatial comparison between wall shear stress measures and porcine arterial endothelial permeability." *American Journal of Physiology-Heart and Circulatory Physiology* 286, no. 5 (2004): H1916-H1922. https://doi.org/10.1152/ajpheart.00897.2003
[42] Budwig, R., D. Elger, H. Hooper, and J. Slippy. "Steady flow in abdominal aortic aneurysm models." *Journal of Biomechanical Engineering* 115, no. 4A (1993): 418-423. https://doi.org/10.1115/1.2895506
[43] Deplano, Valerie, Yannick Knapp, Eric Bertrand, and Emmanuel Gaillard. "Flow behaviour in an asymmetric compliant experimental model for abdominal aortic aneurysm." *Journal of Biomechanics* 40, no. 11 (2007): 2406-2413. https://doi.org/10.1016/j.jbiomech.2006.11.017
[44] Jeong, Jinhee, and Fazle Hussain. "On the identification of a vortex." *Journal of Fluid Mechanics* 285 (1995): 69-94. https://doi.org/10.1017/S0022112095000462
[45] Formaggia, Luca, Alfio Quarteroni, and Allesandro Veneziani, eds. *Cardiovascular Mathematics: Modeling and simulation of the circulatory system*. Vol. 1. Springer Science & Business Media, 2010. https://doi.org/10.1007/978-88-470-1152-6
[46] Malek, Adel M., Seth L. Alper, and Seigo Izumo. "Hemodynamic shear stress and its role in atherosclerosis." *JAMA* 282, no. 21 (1999): 2035-2042. https://doi.org/10.1001/jama.282.21.2035
[47] Boyd, April J., David CS Kuhn, Richard J. Lozowy, and Gordon P. Kulbisky. "Low wall shear stress predominates at sites of abdominal aortic aneurysm rupture." *Journal of Vascular Surgery* 63, no. 6 (2016): 1613-1619. https://doi.org/10.1016/j.jvs.2015.01.040
[48] Qiu, Yue, Ding Yuan, Jun Wen, Yubo Fan, and Tinghui Zheng. "Numerical identification of the rupture locations in patient-specific abdominal aortic aneurysmsusing hemodynamic parameters." *Computer Methods in Biomechanics and Biomedical Engineering* 21, no. 1 (2018): 1-12. https://doi.org/10.1080/10255842.2017.1410796
[49] da Silva, Erasmo Simão, Aldo Junqueira Rodrigues, Erasmo Magalhães Castro de Tolosa, Consuelo Junqueira Rodrigues, Gladys Villas Boas do Prado, and João Carlos Nakamoto. "Morphology and diameter of infrarenal aortic aneurysms: a prospective autopsy study." *Cardiovascular Surgery* 8, no. 7 (2000): 526-532. https://doi.org/10.1016/S0967-2109(00)00060-0
[50] Kelsey, Lachlan J., Janet T. Powell, Paul E. Norman, Karol Miller, and Barry J. Doyle. "A comparison of hemodynamic metrics and intraluminal thrombus burden in a common iliac artery aneurysm." *International Journal for Numerical Methods in Biomedical Engineering* 33, no. 5 (2017): e2821. https://doi.org/10.1002/cnm.2821